Supporting Information

Discrete Organic Phosphorus Signatures are Evident in Pollutant Sources within a Lake Erie Tributary

Brooker, MR[1,2]*; Longnecker, K[3]; Kujawinski, EB[3]; Evert, MH[1,2]; and Mouser, PJ[1,4]*.

[1]Department of Civil, Environmental, and Geodetic Engineering, Ohio State University, Columbus, Ohio 43210, United States
[2]Environmental Science Graduate Program, Ohio State University, Columbus, Ohio 43210, United States
[3]Woods Hole Oceanographic Institution, Department of Marine Chemistry and Geochemistry, Woods Hole, MA 02543, USA
[4]Department of Civil and Environmental Engineering, University of New Hampshire, Durham, New Hampshire 03824, USA

This document includes one Excel file, and 19 pages including additional experimental methodology, 5 figures, and 5 tables including: ESI FT-ICR-MS results (SanduskyMaterialResults.xlsx); solid phase extraction efficiency for wastewater (Figures S1); solid phase extraction of organic phosphorus standards (Figure S2); sample elemental compositions (Figure S3); sample spectra (Figure S4); Venn Euler diagrams of shared molecules between samples (Figure S5); molecular class NOSC values (Figure S6); sample sorption efficiency (Table S1); quality filtering of samples (Table S2); number of peaks per sample (Table S3); Venn count data (Table S4); and formula for potential markers (Table S5).

Methods

Prior to ESI(-) FT-ICR MS analysis, the protocols used for organic matter collection were tested to determine their ability to isolate organic phosphorus compounds. Several organic phosphorus compounds were purchased to be used as reference compounds: 2-aminoethyl phosphonate (2-AEP); fosfomycin (FOM); *n*-hexylphosphonic acid (HexP); glucose-6-phosphate (G6P); phenyl phosphate (PhP); nicotinamide dinucleotide phosphate (reduced, NADH); monopotassium phosphate (PO4); and sodium pyrophosphate (P2O7). Each standard was prepared as a stock 1 mg L^{-1} P solution in DI water. A sample of primary clarifier water was collected from the Southerly Wastewater Plant (Columbus, OH) following the methods described in the manuscript. An initial experiment was designed to determine the carbon, nitrogen and phosphorus retention efficiency of four SPE column types (Agilent Bond Elut): functionalized styrene divinylbenzene (PPL); hydrophobic, bonded silica (C18); polymer anionic exchange (PAX); strong anionic exchange (SAX). While the manufacturer instructions call for the adjustment of samples to a pH 2 for the PPL and C18 columns, the PAX and SAX columns recommend adjusting the sample to a pH 10. The primary clarifier water was used to determine the retention of phosphorus by all four columns, both at pH 2 and pH 10 with duplicates for each column (n=16). Following the determination of pH adjustments, a mixture of the reference organic phosphorus compounds were used to determine the retention of these compounds for each filter at pH 10 using duplicate columns. However, due to observed desorption, the SAX columns were excluded from this subsequent analysis (n=6).

Primary clarifier water was passed through the SPE columns using the methods described in the manuscript. The amount of carbon applied to each column type was determined to meet the maximum sorption capacity. The retention efficiency of NPOC and TDN were determined by

the change in concentration between the influent and effluent of samples as measured with the Shimadzu TOC-V/TN. The retention efficiency of TDP was determined by the change in concentration between the influent and effluent samples using an Agilent ICP-OES.

A 7.5 mg L^{-1} P concentration mixture using equal parts (0.9375 mg L^{-1} P) of the eight phosphorus reference compounds – six organic, and two inorganic – was prepared for further analysis of the SPE columns. The mixture was analyzed using ion chromatography with an AS-11HC column on a Dionex ICS-2100 ion chromatograph (Dionex Corporation, Sunnyvale, CA). The flow rate was set at 1.5 mL/min for 15 min a sample, eluted in a 1-60 mM gradient of KOH at 30°C[1]. This method allowed for the detection of seven out of the eight compounds, with the lone exception being 2-AEP. These samples were made basic (pH 10) using KOH and gravity filtered through three SPE column types in duplicate (n=6). The effluent was collected in combusted glassware and ion chromatography analysis was used to visually detect the presence/absence of the compounds following passage through the solid phase columns.

Collection of Mass Spectrometry Data and Peak Detection

The samples were analyzed with electrospray ionization under the negative ionization mode on a 7T FTICR mass spectrometer (Thermo Fisher Scientific, Waltham, MA USA). The instrument settings were optimized by tuning on the SRFA standard. The samples were infused into the ESI interface at 4 μL min^{-1}, and the instrumental and spray parameters were optimized for each sample. The capillary temperature was set at 250°C, and the spray voltage was between 3.7 and 4 kV. For each sample, 200 scans were collected spanning the 200-1000 *m/z* range. An external calibration mixture (Thermo Calibration Mix; Thermo Fisher Scientific) was used to calibrate the mass accuracy to <1.5 ppm. The target average resolving power was 400,000 at *m/z*

400 (where resolving power is defined as m/Δm 50% where Δm is the width at half-height of peak m).

Individual transients as well as a combined raw file were collected using xCalibur 2.0 (Thermo Fisher Scientific). Transients were co-added and processed with custom-written MATLAB code[2]. Only transients with a total ion current >20% of the maximum value observed in each sample were added, processed with Hanning apodization, and zero-filled prior to fast Fourier transformation. All *m/z* values with a signal:noise ratio > 10 were retained. Spectra were internally re-calibrated using a list of *m/z* values present in the majority of samples resulting in a mass accuracy of < 1 ppm[3]. Individual sample peak lists were then aligned in MATLAB[4]. Formula assignments were made through the custom-built Compound Identification Algorithm at the Wood Hole Oceanographic Institution, as previously described[5, 6].

The nominal oxidation state of carbon (NOSC) for each identified formula was calculated according to the equation of *Boye et al*. (2016). The equation is based on the count of individual atom counts according to equation 1. The distribution of the NOSC values were considered for each molecular classification, using only unique formula (no duplicates between ^{12}C and ^{13}C isotopologues).

$$NOSC = 4 - \frac{4C+H-2O-3N-2S+5P}{C} \qquad \text{(equation 1)}$$

Results & Discussion

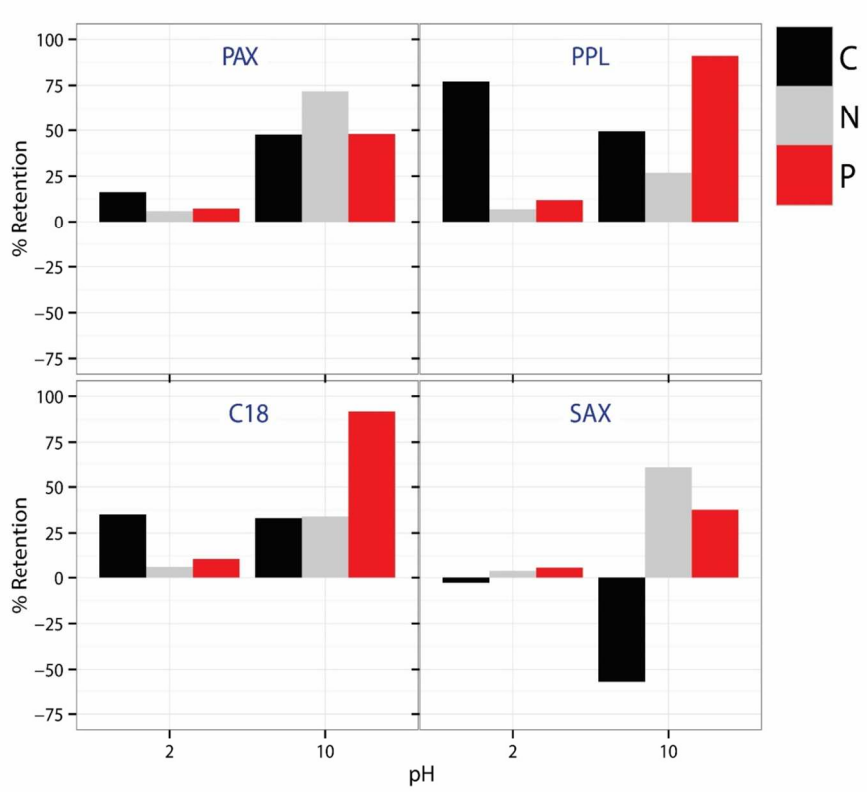

Figure S1. Wastewater primary clarifier water was used to assess the retention of dissolved organic carbon, total dissolved nitrogen, and total dissolved phosphorus by the solid phase extraction materials. Four different resins were tested: PAX, PPL, C18, and SAX. Samples of the wastewater were adjusted to pH 2 or 10 using hydrochloric acid or sodium hydroxide, respectively. The change in concentration was multiplied by the volume which was passed through the filter to estimate the % retention of these elements.

The selection of SPE materials has been principally chosen so that the resulting sample best reproduces the signature that would be observed in the original sample. Previous research has used PPL filters for its broad selectivity of carbon[7]. However, phosphorus represents a minor portion of dissolved organic matter pool. Selective concentration of organic phosphorus compounds enhances their detectability in the organic matter spectrum[8] Our objective was to determine which SPE material and methodology would best suit our needs to retain organic phosphorus compounds. The retention efficiencies of the all four SPE materials had enhanced P recovery when samples were adjusted to a pH 10 (SI Figure S1). Carbon retention displayed

some differences using this method with increased recovery for the PAX column, but a reduction in the carbon recovery for the other three columns. Most notably, the SAX column had an increased carbon concentration in the effluent, and therefore was removed from subsequent analyses. As the majority of phosphorus may have been inorganic in the primary clarifier water, it was important to demonstrate that these columns were retaining organic phosphorus compounds.

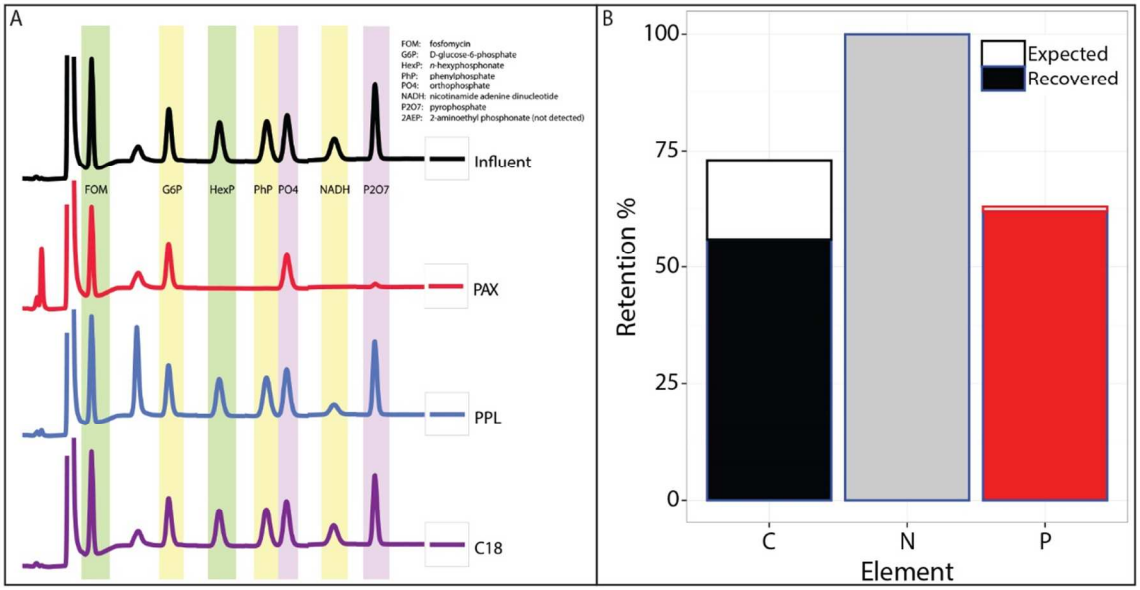

Figure S2. A standard solution consisting of equal parts phosphorus of: (inorganic) orthophosphate, pyrophosphate, (organophosphate) D-glucose-6-phosphate, phenylphosphate, NADH, (organophosphonate) fosfomycin, 2-aminoethyl phosphonate, and *n*-hexylphosphonate was prepared. The sample was basified to a pH 10 and passed through the Plexa-PAX, PPL, and C18 columns. The standard solution was read using ion chromatography before (influent) the eluent was collect from its respective column. The disappearance of a peak has been interpreted as the adsorption of that compound to the SPE column. The 2-aminoethyl phosphonate compound could not be detected using anionic IC. However, the expected retention % assuming complete recovery of 1-aminoethyl phosphonate, hexylphosphonate, phenylphosphate, NADH, and pyrophosphate by the Plexa-PAX filter indicated that this compound also adhered to this filter (e.g., 100% recovery of nitrogen).

The primary clarifier water was likely to contain minerals that could interfere with the interpretation of our results. For instance, the presence of magnesium in the water combined with the pH adjustment could lead to the precipitation of inorganic phosphates[9]. In fact, precipitates were visually observed in the samples prior to filtration. Therefore, using the laboratory phosphorus standards allowed us to detect their retention in the absence of interfering chemicals. Rather than quantifying the change in concentrations, the ion chromatographs were used to identify changes to the presence of particular compounds before and after SPE filtration (SI Figure S2A). The PAX column nearly lacked four of the compounds in its effluent chromatograph: HexP, PhP, NADH, and P2O7. These represented three organic and one inorganic compound. Notably, there was a near complete recovery of nitrogen – as determined by TDN analysis – that could indicate the recovery of the 2-AEP compound (Figure S2B). The determined recovery percent of nitrogen and phosphorus matched the results expected presuming complete recovery of 2-AEP, PhP, NADH, and P2O7. These results confirmed that the PAX column and methodology was adequate for organic phosphorus retention, and therefore this solid phase extraction resin was selected for future analyses.

The DOM of our samples ranged were composed of ≤12.8% DOP. Despite our efforts to enhance organic phosphorus recovery by using the anionic exchange SPE column, the non-manure samples were composed of less organic phosphorus than samples of Lake Superior tributaries[10]. It is noteworthy that we did not discern any retention of organic phosphorus standards by the C18 column, which had been used in the Lake Superior study[10]. Rather than retaining a greater number of phosphorus compounds, it is possible that our method simply enhanced the recovery amounts rather than isolating new compounds. ESI FT-ICR-MS does not measure concentrations so there is no valid way of determining this for our sample set[11].

Additionally, the formula algorithm also has an implicit bias against organic phosphorus in that it preferentially selects formula with the lowest non-oxygen (N+S+P) atom counts[5, 6]. For every phosphorus atom incorporated in a formula, it becomes less likely for that formula to be selected. Formula assignments are made within a 1 ppm error window, meaning that more options are available at higher molecular masses. Supporting this notion of an assignment bias, the organic phosphorus compounds were more often assigned in the lower molecular masses where there were fewer alternatives (data not shown). Our study is a rare instance in which organic phosphorus was the intended focal point of ESI FT-ICR-MS analysis. It would be useful to challenge the existing protocols if this technology is to be applied for other studies centering around organic phosphorus.

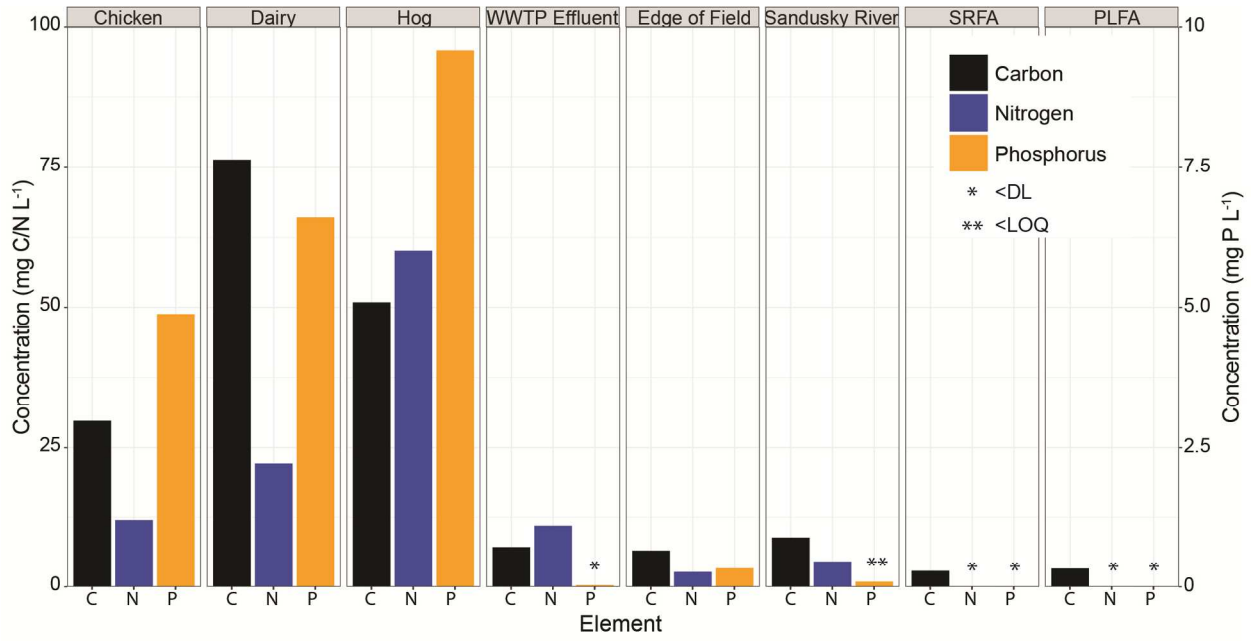

Figure S3. (A) The carbon, nitrogen and phosphorus concentrations were measured as non-purgeable carbon (NPOC), total dissolved nitrogen (TDN); and total dissolved phosphorus (ICP-OES). The detection limit (DL) for N was 0.01 mg N L^{-1}, while it was 0.03 mg P L^{-1} leading to a lower limit of quantification (LOQ) of 0.1 mg P L^{-1}. Concentrations were diluted prior to solid phase extraction.

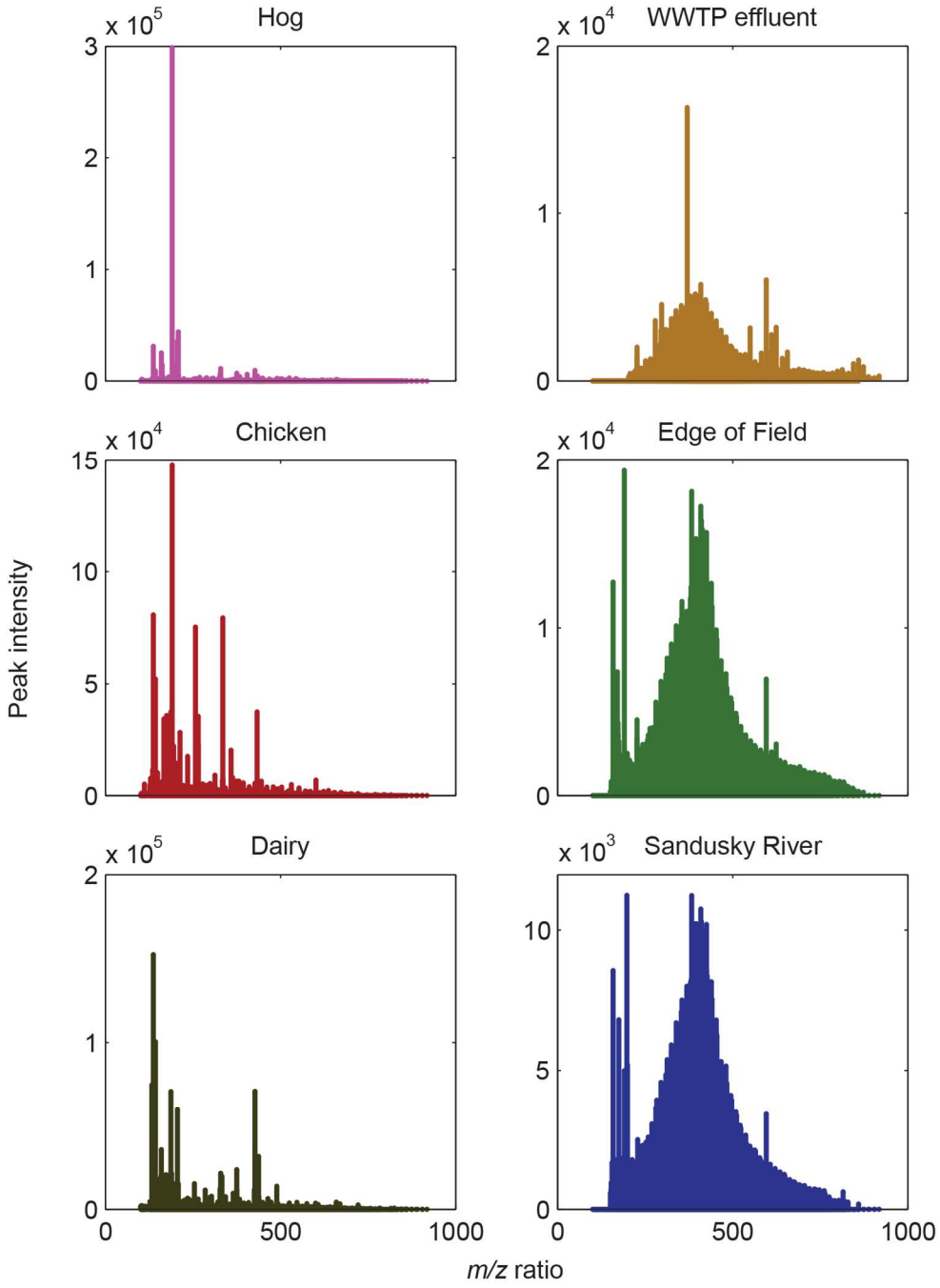

Figure S4. Negative ion mode spectra from DOM from the six watershed samples. The data have been blank-corrected and represent the average peak heights across the two replicates from each sample type.

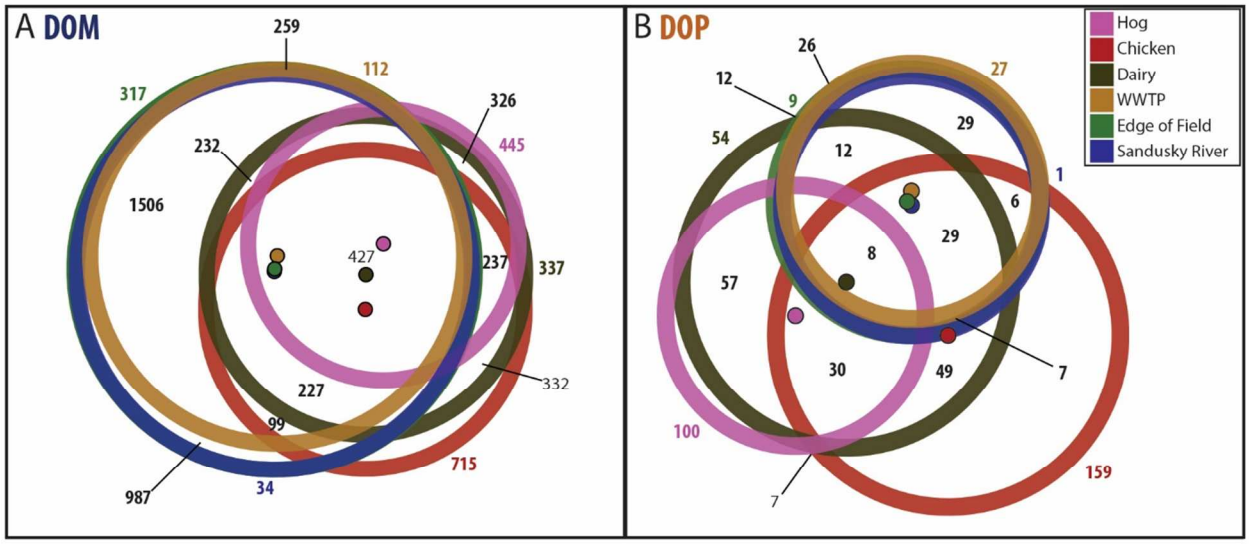

Figure S5. Sample similarity based on presence/absence data. visualized using Euler diagrams for (A) DOM and (B) DOP. The centroid is marked by a small circle with numbers indicating the number of formula shared within an intersection. Not all numbers are indicated but may be found in SI Table S4. The number of unique formula for each sample is color-coded and placed adjacent to that sample's ring.

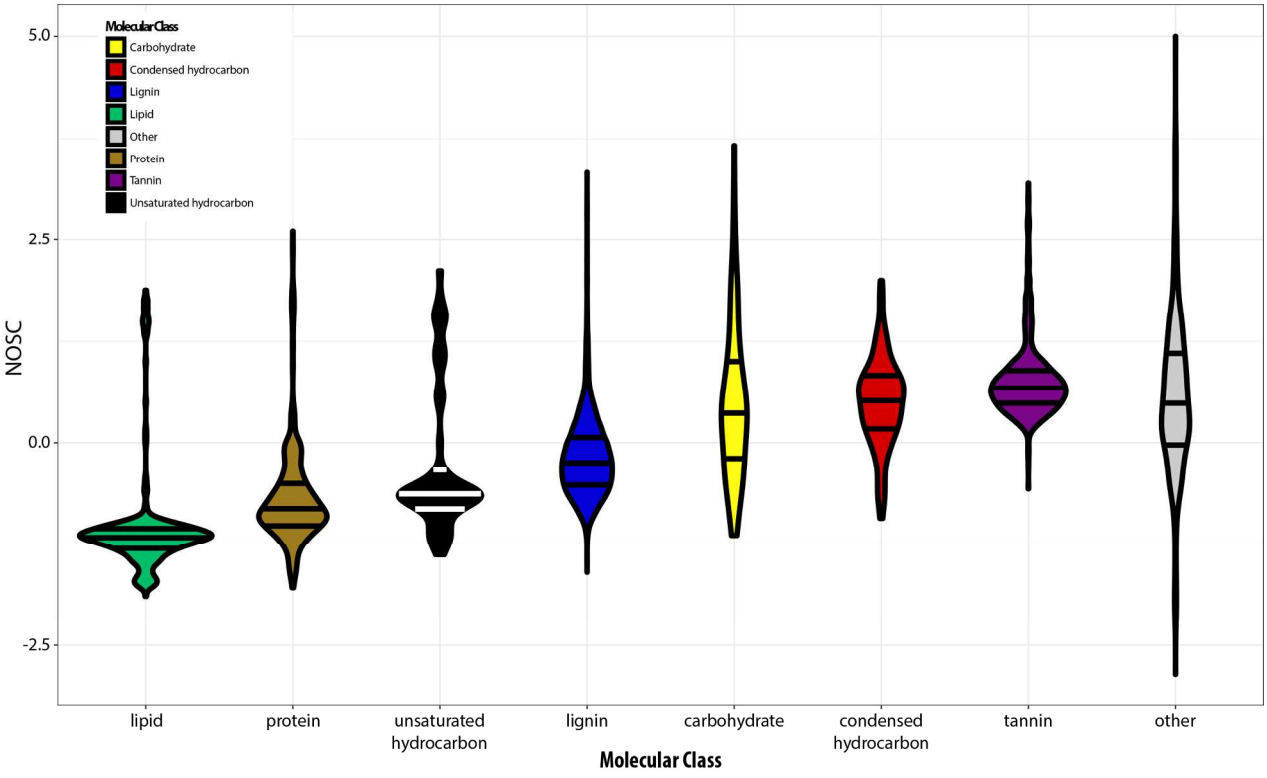

Figure S6. The nominal oxidation state of carbon (NOSC) calculated by molecular class across all samples in this dataset, as visualized in a violin plot. A negative value represents carbon in a reduced state; a positive value represents carbon in an oxidized state; and zero represents carbon which is neutrally charged.

Table S1. Adsorption efficiency across samples using the Bond Elut PAX solid phase extraction resin. Carbon was measured using non-purgeable organic carbon, while nitrogen and phosphorus were measured as the change in concentrations following sample dilution and after passing through the solid phase extraction columns. Values below the limit of quantification (10 µg N L^{-1}, 100 µg P L^{-1}) are reported as estimates. Where effluent values were above influent, values are reported as <0%. BDL indicates that the N or P concentration was below the detection limit.

Sample	Replicate	C	N	P
Chicken	replicate 1	18%	26%	<0%
	replicate 2	19%	28%	15%
Dairy	replicate 1	20%	13%	6.4%
	replicate 2	8%	31%	5.2%
Hog	replicate 1	10%	41%	<0%
	replicate 2	19%	41%	<0%
WWTP Effluent	replicate 1	44%	32%	est. 100%
	replicate 2	12%	32%	est. 97%
Edge of Field	replicate 1	21%	6%	est. 17%
	replicate 2	16%	7%	est. 9.1%
Sandusky River	replicate 1	36%	25%	est. 59%
	replicate 2	28%	33%	est. 76%
SRFA	-	41%	BDL	BDL
PLFA	-	42%	BDL	BDL

Table S2. ESI(-) FT-ICR-MS analysis detected a total of 14637 peaks, spread across the samples and replicates. The data was quality filtered by removing peaks detected in the DI procedural blank; the extraction solvent; singletons (detected in only 1 sample of the entire dataset); and peaks which had no assigned formula. The reproducibility was determined between sample replicates (shared#/mean#).

				Hog		Chicken		Dairy		Wastewater		Edge of field		Sandusky River		NOM	
Processing	Total	DI	Solvent	1	2	1	2	1	2	1	2	1	2	1	2	PLFA	SRFA
All Detected Peaks	14637	3014	534	2497	2352	3452	2493	3519	1626	2388	3602	4449	4702	4169	3154	3412	3707
Remove Peaks in Blank	11633	-	377	2094	2053	3219	2312	3215	1232	2245	3341	4338	4483	3983	3023	3262	3415
Remove Peaks in Solvent	11246	-	-	1983	1931	3098	2200	3070	1128	2171	3270	4260	4396	3895	2939	3146	3325
Removed Singleton Peaks	7438	-	-	1673	1700	2364	2072	2476	995	2070	3096	3979	4254	3853	2815	2630	3027
Assigned Formula	**7250**	**-**	**-**	**1590**	**1625**	**2315**	**2021**	**2444**	**964**	**2046**	**3071**	**3974**	**4220**	**3846**	**2798**	**2622**	**3021**
Reproducibility between sample replicates				88%		88%		68%		81%		90%		85%		-	

Table S3. ESI(-) FT-ICR-MS analysis provided peaks which were assigned formulas with C/H/O/N/P/S elements. The distribution of the *m/z* values detected in each sample were distributed across 8 formula classes. The numbers of formula are printed for each sample replicate with the number in bold indicating the total number detected in the combined samples.

		Hog		Chicken		Dairy		WWTP Effluent		Edge of field		Sandusky River		NOM	
	Total	1	2	1	2	1	2	1	2	1	2	1	2	PLFA	SRFA
CHO	**3981**	772	857	824	801	1139	475	1700	2374	3037	3190	2913	2154	**1749**	**2727**
		906		**908**		**1144**		**2413**		**3356**		**2924**			
CHON	**2198**	502	466	1047	814	923	276	239	479	732	827	769	549	**751**	**119**
		550		**1064**		**927**		**488**		**903**		**811**			
CHOP	**394**	111	99	172	150	203	112	57	126	117	117	109	75	**70**	**78**
		119		**179**		**207**		**129**		**132**		**111**			
CHOS	**254**	62	68	75	69	89	37	7	40	68	35	21	2	**38**	**74**
		72		**82**		**93**		**40**		**75**		**22**			
CHONP	**147**	50	44	81	79	30	23	9	19	7	18	12	6	**3**	**5**
		53		**83**		**35**		**19**		**18**		**13**			
CHONS	**149**	39	46	66	61	37	20	22	19	10	19	15	9	**8**	**12**
		47		**69**		**40**		**28**		**22**		**16**			
CHOPS	**62**	30	24	24	23	18	14	2	5	0	3	2	0	**1**	**2**
		30		**25**		**18**		**5**		**3**		**2**			
CHONPS	**65**	24	21	26	24	5	7	10	9	3	11	5	3	**2**	**4**
		26		**26**		**9**		**14**		**13**		**6**			
Total	**7250**	1590	1625	2315	2021	2444	964	2046	3071	3974	4220	3846	2798	**2622**	**3021**
		1803		**2436**		**2473**		**3136**		**4522**		**3905**			

Table S4. The Venn counts used to produce the Euler diagrams plotted in Figure 4. The samples columns are binary (0 not included; 1 included) with the numbers in the DOM and DOP columns indicating the number of formula for that group of samples.

Hog	Chicken	Dairy	WWTP Effluent	Edge of Field	Sandusky River	DOM	DOP
0	0	0	0	0	1	34	1
0	0	0	0	1	0	317	9
0	0	0	0	1	1	987	12
0	0	0	1	0	0	112	27
0	0	0	1	0	1	26	2
0	0	0	1	1	0	259	26
0	0	0	1	1	1	1506	29
0	0	1	0	0	0	337	54
0	0	1	0	0	1	4	2
0	0	1	0	1	0	17	0
0	0	1	0	1	1	17	1
0	0	1	1	0	0	15	3
0	0	1	1	0	1	1	0
0	0	1	1	1	0	26	1
0	0	1	1	1	1	232	12
0	1	0	0	0	0	715	159
0	1	0	0	0	1	4	0
0	1	0	0	1	0	9	0
0	1	0	0	1	1	59	4
0	1	0	1	0	0	1	1
0	1	0	1	0	1	1	0
0	1	0	1	1	0	6	1
0	1	0	1	1	1	99	6
0	1	1	0	0	0	332	49
0	1	1	0	0	1	4	1
0	1	1	0	1	0	18	0
0	1	1	0	1	1	61	7
0	1	1	1	0	0	5	4
0	1	1	1	0	1	1	0
0	1	1	1	1	0	5	0
0	1	1	1	1	1	227	29
1	0	0	0	0	0	445	100
1	0	0	0	0	1	3	1
1	0	0	0	1	0	8	1
1	0	0	0	1	1	3	0

1	0	0	1	0	0	5	1
1	0	0	1	0	1	0	0
1	0	0	1	1	0	9	3
1	0	0	1	1	1	35	8
1	0	1	0	0	0	326	57
1	0	1	0	0	1	1	0
1	0	1	0	1	0	8	0
1	0	1	0	1	1	1	0
1	0	1	1	0	0	7	1
1	0	1	1	0	1	0	0
1	0	1	1	1	0	11	0
1	0	1	1	1	1	52	4
1	1	0	0	0	0	69	7
1	1	0	0	0	1	1	0
1	1	0	0	1	0	1	1
1	1	0	0	1	1	6	0
1	1	0	1	0	0	1	0
1	1	0	1	0	1	1	0
1	1	0	1	1	0	0	0
1	1	0	1	1	1	45	0
1	1	1	0	0	0	237	30
1	1	1	0	0	1	17	1
1	1	1	0	1	0	14	0
1	1	1	0	1	1	49	4
1	1	1	1	0	0	12	1
1	1	1	1	0	1	1	0
1	1	1	1	1	0	8	0
1	1	1	1	1	1	427	8

Table S5. List of potential marker formulas found in source and Sandusky River samples. The mass to charge (*m/z*) ratios were used to identify a molecular formula. C13 indicates the presence (1) or absence (0) of a single ^{13}C isotope in the formula. The relative peak height for the *m/z* values in the samples is provided, and - signifies that the *m/z* value was not detected for that sample.

m/z	Formula	C13	Hog	Chicken	Dairy	WWTP Effluent	Edge of field	Sandusky River
432.0675772	C20H20O6NPS	-	-	-	2.14E-04	-	-	6.62E-05
464.1477252	C22H28O8NP	-	-	-	3.78E-04	-	-	8.25E-05
277.1433072	C10H23O3N4P	-	-	1.10E-04	4.24E-04	-	-	3.39E-05
276.0724817	C11H17O6P	1	2.54E-04	6.89E-04	8.44E-04	-	-	4.09E-05
408.2239451	C19H37O7P	1	-	-	-	7.22E-05	-	5.76E-05
376.0885573	C15H21O9P	1	-	-	-	-	1.13E-04	6.34E-05
420.0783553	C16H21O11P	1	-	-	-	-	9.02E-05	4.77E-05
420.1147941	C17H25O10P	1	-	-	-	-	8.38E-05	5.16E-05
430.0779524	C21H19O8P	1	-	-	-	-	9.68E-05	5.18E-05
434.0940188	C17H23O11P	1	-	-	-	-	8.76E-05	5.08E-05
502.1565882	C22H31O11P	1	-	-	-	-	8.25E-05	5.05E-05
406.135515	C17H27O9P	1	-	-	7.44E-05	-	8.54E-05	4.73E-05
332.0623426	C13H17O8P	1	-	2.05E-04	-	-	9.30E-05	4.94E-05
392.0834377	C15H21O10P	1	-	2.02E-04	-	-	7.88E-05	4.62E-05
302.0881438	C13H19O6P	1	-	2.59E-04	4.41E-04	-	8.02E-05	4.26E-05
304.0674032	C12H17O7P	1	-	5.06E-04	4.50E-04	-	7.36E-05	4.10E-05
318.0830637	C13H19O7P	1	-	5.92E-04	1.91E-04	-	8.09E-05	4.78E-05
330.0830667	C14H19O7P	1	-	2.01E-04	1.47E-04	-	1.36E-04	1.38E-04
332.0987091	C14H21O7P	1	-	2.57E-04	1.13E-04	-	9.82E-05	4.42E-05
362.1092918	C15H23O8P	1	-	6.35E-05	7.52E-05	-	9.24E-05	4.80E-05
275.0260021	C9H13O4N2PS	-	4.46E-04	1.31E-04	7.34E-04	-	4.33E-05	8.45E-05
294.0619326	C14H15O5P	1	3.39E-04	4.22E-04	6.09E-04	-	9.19E-05	1.27E-04
320.0775812	C16H17O5P	1	3.64E-04	1.78E-04	4.03E-04	-	4.06E-05	4.53E-05
421.236256	C20H39O7P	-	3.57E-04	1.97E-04	1.33E-03	-	3.64E-05	7.27E-05
372.1664215	C18H29O6P	1	-	-	-	3.03E-04	1.33E-04	1.76E-04
386.1820806	C19H31O6P	1	-	-	-	2.22E-04	9.86E-05	1.10E-04
388.1613368	C18H29O7P	1	-	-	-	2.70E-04	1.54E-04	1.69E-04
402.1769532	C19H31O7P	1	-	-	-	2.09E-04	1.05E-04	1.38E-04
403.1165379	C17H25O9P	-	-	-	-	1.00E-04	9.28E-05	4.57E-05
413.100923	C18H23O9P	-	-	-	-	1.10E-04	8.84E-05	3.93E-05
416.1926161	C20H33O7P	1	-	-	-	1.74E-04	1.04E-04	1.08E-04
417.095797	C17H23O10P	-	-	-	-	9.12E-05	4.37E-05	4.11E-05
418.0990897	C17H23O10P	1	-	-	-	7.87E-05	1.75E-04	1.74E-04
418.1718666	C19H31O8P	1	-	-	-	7.17E-05	9.78E-05	5.75E-05
429.1322172	C19H27O9P	-	-	-	-	1.18E-04	7.46E-05	3.66E-05

488.1773569	C22H33O10P	1	-	-	-	5.45E-05	8.69E-05	4.83E-05
344.1351164	C16H25O6P	1	-	-	8.28E-05	2.60E-04	1.41E-04	1.60E-04
370.1507808	C18H27O6P	1	-	-	9.10E-05	3.58E-04	1.57E-04	2.28E-04
372.1300277	C17H25O7P	1	-	-	9.49E-05	3.00E-04	2.15E-04	2.31E-04
382.1507627	C19H27O6P	1	-	-	1.11E-04	3.36E-04	2.01E-04	2.34E-04
384.166397	C19H29O6P	1	-	-	9.51E-05	2.90E-04	1.77E-04	2.08E-04
399.0852169	C17H21O9P	-	-	-	4.55E-04	7.87E-05	8.40E-05	3.89E-05
414.176966	C20H31O7P	1	-	-	7.62E-05	3.70E-04	2.13E-04	2.34E-04
458.1668009	C21H31O9P	1	-	-	7.86E-05	2.57E-04	1.63E-04	1.92E-04
484.1824486	C23H33O9P	1	-	-	7.72E-05	2.19E-04	1.65E-04	2.03E-04
360.130038	C16H25O7P	1	-	7.45E-05	-	2.13E-04	1.59E-04	1.88E-04
456.1147265	C20H25O10P	1	-	7.61E-05	-	2.90E-04	2.52E-04	2.77E-04
342.1194474	C16H23O6P	1	-	1.67E-04	1.17E-04	3.47E-04	1.65E-04	2.11E-04
344.0987134	C15H21O7P	1	-	1.87E-04	1.48E-04	8.20E-05	1.40E-04	1.73E-04
350.0881719	C17H19O6P	1	-	2.26E-04	4.02E-04	2.42E-04	1.37E-04	1.56E-04
354.0830662	C16H19O7P	1	-	3.05E-04	1.23E-04	2.32E-04	2.25E-04	2.50E-04
356.0623315	C15H17O8P	1	-	3.92E-04	1.82E-04	6.87E-05	2.34E-04	2.79E-04
356.1351082	C17H25O6P	1	-	6.45E-05	1.11E-04	2.68E-04	1.47E-04	1.73E-04
358.1143977	C16H23O7P	1	-	6.54E-05	1.13E-04	2.56E-04	2.25E-04	2.31E-04
368.0987153	C17H21O7P	1	-	2.04E-04	1.38E-04	3.00E-04	2.26E-04	2.86E-04
370.1143768	C17H23O7P	1	-	1.06E-04	1.22E-04	2.99E-04	2.25E-04	2.70E-04
380.098741	C18H21O7P	1	-	1.02E-04	3.92E-04	3.54E-04	2.54E-04	3.08E-04
382.1143594	C18H23O7P	1	-	2.00E-04	1.27E-04	3.69E-04	2.99E-04	3.32E-04
396.1300303	C19H25O7P	1	-	2.24E-04	1.46E-04	4.39E-04	3.31E-04	3.48E-04
398.1456726	C19H27O7P	1	-	2.14E-04	1.23E-04	4.31E-04	3.05E-04	3.31E-04
410.109275	C19H23O8P	1	-	1.94E-04	1.33E-04	4.50E-04	3.60E-04	4.13E-04
410.145669	C20H27O7P	1	-	2.18E-04	1.17E-04	4.47E-04	2.96E-04	3.49E-04
412.1613237	C20H29O7P	1	-	1.75E-04	1.18E-04	4.35E-04	2.96E-04	3.38E-04
430.1354991	C19H27O9P	1	-	6.31E-05	1.10E-04	2.77E-04	2.47E-04	2.50E-04
440.119842	C20H25O9P	1	-	1.73E-04	9.72E-05	3.63E-04	3.13E-04	3.41E-04
440.1562514	C21H29O8P	1	-	1.85E-04	1.13E-04	3.42E-04	2.81E-04	3.06E-04
426.067739	C18H19O10P	1	3.78E-04	-	1.20E-03	2.03E-04	2.97E-04	3.55E-04
296.0775853	C14H17O5P	1	2.26E-04	5.66E-04	4.98E-04	5.81E-05	1.02E-04	6.58E-05
322.0932496	C16H19O5P	1	5.06E-04	2.23E-04	8.40E-04	7.76E-05	1.00E-04	1.61E-04
336.1088903	C17H21O5P	1	1.91E-04	2.01E-04	1.31E-04	2.15E-04	9.13E-05	1.17E-04
366.0830953	C17H19O7P	1	6.32E-04	2.19E-04	1.42E-03	2.65E-04	1.95E-04	2.55E-04
384.0936035	C17H21O8P	1	2.21E-04	3.47E-04	8.02E-04	2.89E-04	3.47E-04	3.64E-04

References

1. Brooker, M.R.; Bohrer, G.; Mouser, P.J. Variations in potential CH_4 flux and CO_2 respiration from freshwater wetland sediments that differ by microsite location, depth and temperature. *Ecological Engineering* **2014,** *72* (The Olentangy River Wetland Research Park: Two Decades of Research on Ecosystem Services), 84-94; http://dx.doi.org/10.1016/j.ecoleng.2014.05.028.

2. Southam, A.D.; Payne, T.G.; Cooper, H.J.; Arvanitis, T.N.; Viant, M.R. Dynamic range and mass accuracy of wide-scan direct infusion nanoelectrospray Fourier transform ion cyclotron resonance mass spectrometry-based metabolomics increased by the spectral stitching method. *Anal. Chem.* **2007,** *79* (12), 4595-4602; http://dx.doi.org/10.1021/ac062446p.

3. Bhatia, M.P.; Das, S.B.; Longnecker, K.; Charette, M.A.; Kujawinski, E.B. Molecular characterization of dissolved organic matter associated with the Greenland ice sheet. *Geochim. Cosmochim. Acta* **2010,** *74* (13), 3768-3784; http://dx.doi.org/10.1016/j.gca.2010.03.035.

4. Mantini, D.; Petrucci, F.; Pieragostino, D.; Del Boccio, P.; Di Nicola, M.; Di Ilio, C.; Federici, G.; Sacchetta, P.; Comani, S.; Urbani, A. LIMPIC: a computational method for the separation of protein MALDI-TOF-MS signals from noise. *BMC Bioinformatics* **2007,** *8* (1), 1; http://dx.doi.org/10.1186/1471-2105-8-101.

5. Kujawinski, E.B.; Behn, M.D. Automated analysis of electrospray ionization Fourier transform ion cyclotron resonance mass spectra of natural organic matter. *Anal. Chem.* **2006,** *78* (13), 4363-4373; https://dx.doi.org/10.1021/ac0600306.

6. Kujawinski, E.B.; Longnecker, K.; Blough, N.V.; Del Vecchio, R.; Finlay, L.; Kitner, J.B.; Giovannoni, S.J. Identification of possible source markers in marine dissolved organic matter using ultrahigh resolution mass spectrometry. *Geochim. Cosmochim. Acta* **2009,** *73* (15), 4384-4399; https://dx.doi.org/10.1016/j.gca.2009.04.033.

7. Ohno, T.; Ohno, P.E. Influence of heteroatom pre-selection on the molecular formula assignment of soil organic matter components determined by ultrahigh resolution mass spectrometry. *Analytical and Bioanalytical Chemistry* **2013,** *405* (10), 3299-3306; https://doi.org/10.1007/s00216-013-6734-3.

8. Cooper, W.T.; Llewelyn, J.M.; Bennett, G.L.; Salters, V.J.M. Mass spectrometry of natural organic phosphorus. *Talanta* **2005,** *66* (2), 348-358; http://dx.doi.org/10.1016/j.talanta.2004.12.028.

9. Karl, David M.,Tien, Georgia, MAGIC: A sensitive and precise method for measuring dissolved phosphorus in aquatic environments. *LNO Limnology and Oceanography* **1992,** *37* (1), 105-116; https://doi.org/10.4319/lo.1992.37.1.0105.

10. Minor, E.C.; Steinbring, C.J.; Longnecker, K.; Kujawinski, E.B. Characterization of dissolved organic matter in Lake Superior and its watershed using ultrahigh resolution mass spectrometry. *Org. Geochem.* **2012,** *43*, 1-11; https://dx.doi.org/10.1016/j.orggeochem.2011.11.007.

11. Kamga, A.W.; Behar, F.; Hatcher, P.G. Quantitative Analysis of Long Chain Fatty Acids Present in a Type I Kerogen Using Electrospray Ionization Fourier Transform Ion Cyclotron Resonance Mass Spectrometry: Compared with BF_3/MeOH Methylation/GC-FID. *Journal of The American Society for Mass Spectrometry* **2014,** *25* (5), 880-890; http://dx.doi.org/10.1007/s13361-014-0851-x.